Journal of Applied Geophysics 210 (2023) 104924

Contents lists available at ScienceDirect

Journal of Applied Geophysics

journal homepage: www.elsevier.com/locate/jappgeo

Improving tailings dam risk management by 3D characterization from resistivity tomography technique: Case study in São Paulo – Brazil

Lorena Andrade Oliveira [a,*], Marco Antonio Braga [a], Guilherme Prosdocimi [b], Alan de Souza Cunha [a], Leonardo Santana [a], Filipa da Gama [a]

[a] *Federal University of Rio de Janeiro, Rio de Janeiro, Rio de Janeiro, Brazil*
[b] *Federal University of Ouro Preto, Ouro Preto, Minas Gerais, Brazil*

A R T I C L E I N F O

Keywords:
Geo-electrical method
Geotechnics
Tailings dam
Resistivity tomography
Dam operational safety

A B S T R A C T

Tailings dams are traditionally monitored by routine visual inspections combined with the use of instruments such as piezometers, topographical landmarks, and water level indicators. As they are structures that have high potential damage associated, the use of robust investigation methods is essential to ensure the operational safety of these dams. Geoelectrical methods have been successful in mapping humid zones inside the tailings dam structures, using the proper acquisition parameters and data sampling that these methods allow. This is a promising approach to investigating a tailings dam with a heterogeneous embankment made of limestone tailings, that has been in operation for 50 years in São Paulo state, Brazil. Considering its structural complexity, electrical resistivity sections were acquired with a tight profile spacing – of 10 to 15 m, processed, and modeled by applying a specific workflow. The Electrical Resistivity Tomography (ERT) operational workflow applied to the dataset obtained from two field campaigns, conducted in the embankment and the right abutment of the dam, performed well in mapping possible high water content zones inside the structure, defining a relevant element for the risk assessment. For this purpose, compartmentalization of the resistivity ranges, and three-dimensional modeling techniques were used, both constrained by the geotechnical instruments of the structure. The embankment campaign mapped zones of attention in the right abutment driving the decision to perform a follow-up survey dedicated to this region. The right abutment campaign mapped zones of high resistivity, associated with the natural terrain, composed of sandy soils, saprolite, and rock, as well as zones of low resistivity related to high moisture content regions. The geometry of these conductive zones made it possible to infer the depth of the water table in the region between the direct measurements from the instrumentation and to model zones with low resistivity values. The 3D modeling revealed that part of the conductive zones, present in the right abutment and extending to the embankment indicate a possible contribution of moisture from the natural terrain towards the embankment of the dam. Thus, the achieved results demonstrated that 3D modeling applied to the combination of the geotechnical and geophysical datasets contributes to expanding the knowledge of the internal structure of the dam and consequently the safety of the operations, especially where there is no instrumentation, improving the tailings dam risk management.

1. Introduction

The mining industry traditionally generates large amounts of waste, which need proper storage and disposal. For this purpose, containment structures, called tailings dams and stockpiles, are built and need to be monitored because of the vast areas they may disturb and the possible toxicity of the materials they retain (Vick, 1990).

According to Azam and Li (2010), tailings dams are structures far more vulnerable to failure than dams built for other purposes. Some of the reasons listed by the authors are based on their construction materials (largely, residues from mining) and for suffering successive raisings throughout their operation, causing the failure rate of these structures to be many times higher in comparison to water-retention dams. In addition to being more vulnerable, they often have a high potential for damage, which, in the event of a failure, can lead to major social and environmental impacts.

* Corresponding author.
E-mail address: oliveiralorena@ufrj.br (L.A. Oliveira).

https://doi.org/10.1016/j.jappgeo.2023.104924
Received 20 June 2021; Received in revised form 6 October 2022; Accepted 3 January 2023
Available online 7 January 2023

Due to two recent major episodes of tailings dams failure in Brazil, in 2015 and 2019, associated with old iron-ore mines (de Oliveira Neves et al., 2016; Rotta et al., 2020), mining companies have been reviewing the operational challenge of having to dispose of such a large amount of waste without compromising the safety of these containment structures. For this reason, tailings dams have become the center of technical discussions, aimed at improving the practices for characterizing the structure and its monitoring, preventing new accidents. In the 21st century, there is a tendency to build more sustainable structures to store the mining waste, using less fresh water and allowing for reutilization of the tailings, either from re-mining or backfilling depleted open pit mines (Breitenbach, 2010), but there are still many mines in operation that use typical tailings dams, composed of a starter dyke and successive raisings, that need constant monitoring. These structures are usually monitored through instruments and routine visual inspections (e.g. Vick, 1990; Fell et al., 2015). Recently, techniques using radar and/or laser scanners, images acquired by drones and satellites, and video monitoring are being used to monitor, superficially, deformations of the dam slopes (Scaioni et al., 2018). These methodologies comply with what is proposed and are of paramount importance for monitoring these structures. However, these methods measure variations in a localized and/or superficial way, not being able to detect anomalies in depth. Thus, more far-reaching methods were demanded regarding the characterization and diagnosis of these structures, bringing Geophysics into the spotlight. The application of geophysical methods, such as Electrical Resistivity Tomography (ERT) to dams is not a novelty (e.g. Bogoslovsky and Ogilvy, 1970; Butler, 1984; Johansson and Dahlin, 1996; Titov et al., 2000; Sjödahl et al., 2005).

Works such as the one published by Mailani (2006) state that electrical resistivity, associated with the Spontaneous Potential (SP) method, has a great capacity to detect anomalous infiltrations and internal erosion processes, highlighting the importance of mapping high water content zones inside dam structures. Recently, numerous authors from all over the world have published studies on the application of the electrical resistivity method to several types of dams, e.g. Al-Fares (2014) used ERT to study a leakage in an earth dam in Syria, Fata et al. (2021) investigated seepage patterns in an earth dam in Indonesia, HIMI, M., et al. (2016) applied the method to leakage detection in a dam in Spain, and Martínez et al. (2021) examined the internal structure of a tailings dam and pond in Spain. The combination of several geophysical, geotechnical, and geochemical methods has also been under recent scrutiny, as published by Sentenac et al. (2017, 2018) and Rey et al. (2021), among many other authors.

Although the applicability is not new, the use of the electrical resistivity method as an operational tool for the risk management of these structures is recent in Brazil. Researchers from IPT (São Paulo State Technological Research Institute) have recently published several studies on the application of several geophysical methods, including ERT to look into the internal structure of earthfill dams (e.g. Souza et al., 2016; Malagutti Filho et al., 2018a, 2018b; Guireli Netto et al., 2019; Guireli Netto et al., 2020).

Albuquerque et al. (2019), Oliveira (2018), Rocha et al. (2019), and Rodrigues (2018) demonstrated the applicability of shallow geophysical methods such as electrical resistivity, Spontaneous Potential (SP), and Ground Penetrating Radar (GPR). These methods were employed to characterize and refine the existing knowledge of tailings dams belonging to mining complexes in the states of São Paulo and Minas Gerais - Brazil. In this work, we will propose an operational workflow to infer high-water content zones using 3D modeling and also to map zones of attention in these structures by using detailed ERT surveying. ERT is proven as an efficient tool to infer humidity. However, its adoption as an operational procedure still depends on the new guidelines to make viable its routine use in risk management procedures.

The object of this study is the application of an ERT operational workflow to improve the risk management of a tailings dam built to receive waste from a phosphate mine.

2. Study area

The study area is geologically located in the Jacupiranga Alkaline Complex, which is mostly composed of two ultramafic intrusions: dunites to the north and clinopyroxenites to the south. Subordinate alkaline rocks and other lithologies are present in the complex in smaller volumes (Melcher, 1954). The B1 Dam belongs to the facilities of a large minerochemical complex, the Cajati complex, located in the southwestern portion of São Paulo State, very close to the border with Parana State. The primary activity of the complex is the extraction of apatite (open-pits), which occurs in carbonatites inserted in clinopyroxenites, locally known as Jacupiranguitos (Derby, 1891). From the apatite ore, sulfuric acid, phosphoric acid, phosphate rock, and dicalcium phosphate are produced. The tailings of this process are composed of calcite (66.6%), dolomite (23.9%), apatite (7.2%), and mica (1.2%). The main purposes of the dam are slurry retention and water clarification. The dam is operating since 1973 and was built through successive raisings, in compacted soil and limestone tailings. A combination of downstream, centerline, and upstream methods were used as constructive methods. Fig. 1 depicts the dam's main components as well as a typical section showing the embankment's main constituent materials.

The construction of the B1 Dam began in 1973 with a starter dyke about 15 m high, built with compacted clay, with a downstream rockfill. A layer of alluvial soil, 1 to 2 m thick, with clayey characteristics and soft consistency, covering the region, was not removed for the construction of the starter dike.

Subsequently, it underwent successive small raisings (Albuquerque et al., 2019) resulting in a zoned massif with an impermeable upstream zone (clay septum), with the downstream and upstream parts built with permeable material consisting of limestone tailings. Fig. 1 shows a section in the center of the dam massif where it is possible to see the complexity of the structure and also to observe the presence of a vertical sand filter associated with a drainage blanket formed by crushed gravel that is interconnected to the rockfill of the toe drain of the structure. This internal drainage system was built during the raising of the structure to an elevation of 55.5 m. In the latest raising, this system was not extended. There is also a longitudinal sand filter in the dam axis at an elevation of 71 m. The downstream face of the dam's slope is protected by sterile Jacupiranguito gravel and grass vegetation. The surface drainage system is made up of trapezoidal open concrete channels installed on berms along the slopes and on the massif's sides. Colluvial soil with a clayey texture and consistency ranging from soft to medium, with an approximate thickness of 4 m, covers the region of the structure's abutments. There is residual Jacupiranguito soil beneath the colluvial soil, with texture ranging from clayey-silty, micaceous of medium to hard consistency in the upper portion, and silty-sandy, micaceous texture, with fragments of altered rock ranging from compact to very compact in depth.

3. Materials and methods

3.1. Data acquisition

Due to the dam's age and its structural complexity, the need for imaging in depth was identified by the company that operates the dam, and given the large applicability of the ERT method in dam investigations, it was chosen for the embankment campaign as a way of expanding the knowledge on the dam, especially about uncontrolled seepage inside the embankment and abutments. In 2017, the first geophysical investigation was carried out by a contractor. Eight sections were acquired (L01 to L08) parallel to the crest (Fig. 2), with spacing between lines ranging from 10 to 15 m, totalizing 2215 m of data acquisition. The second campaign was planned and executed, in 2019, as a follow-up work to the first one. It consisted of six more sections (L15 - L20) in the region of the right abutment of the dam, using the 2D resistivity imaging (ERT) method and the same spacing between sections,

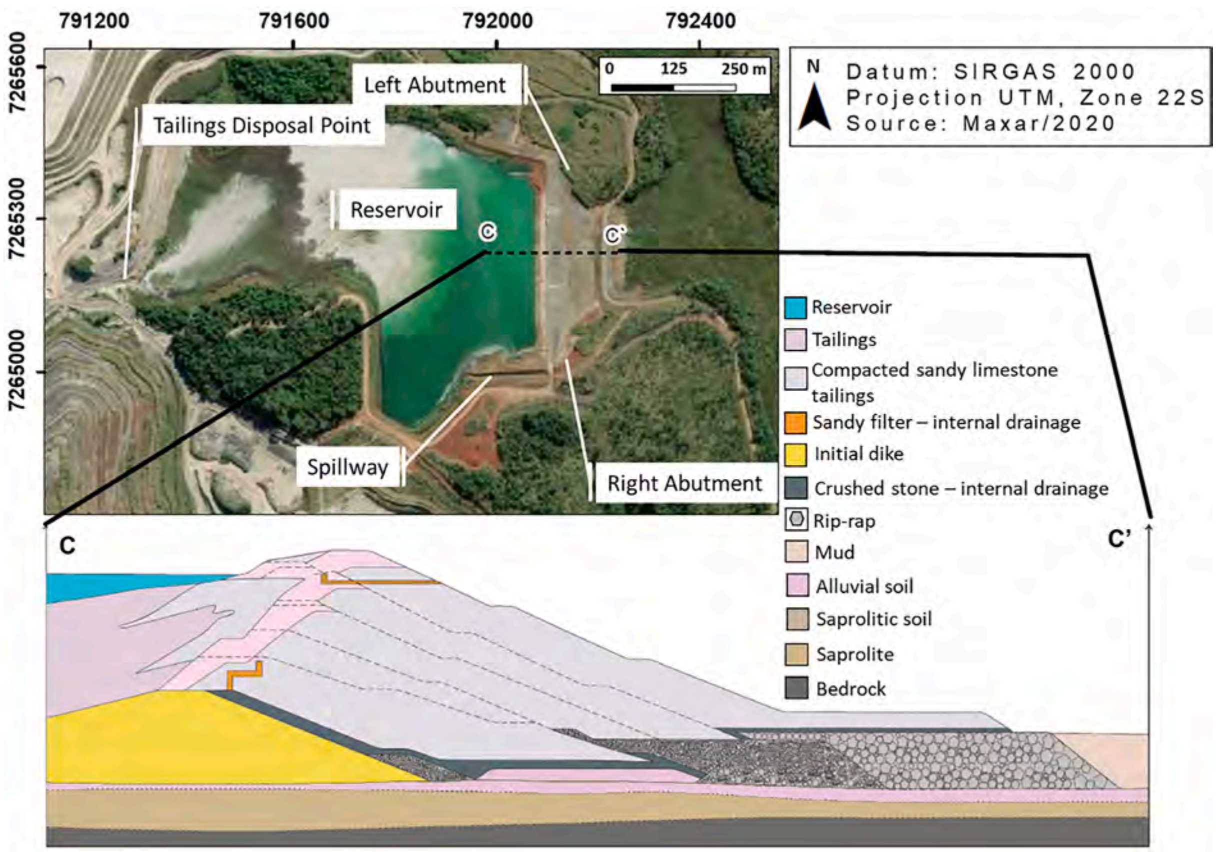

Fig. 1. Illustration of the general arrangement of the B1 Dam, indicating its main structural components. C-C′ typical section of the structure is shown below.

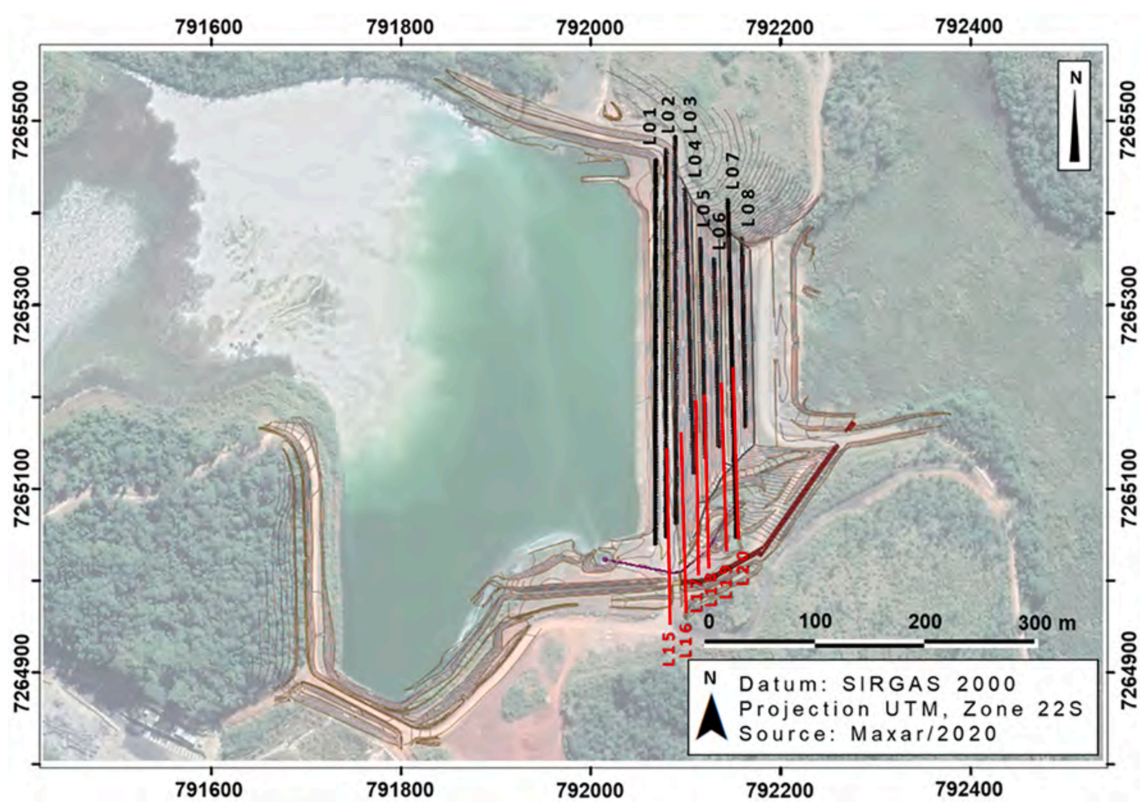

Fig. 2. Location of the electrical resistivity surveys carried out at the dam, covering sections L01 to L08 of the first campaign in black (July to September 2017) and L15 to L20 of the right abutment campaign in red (February 2019). (For interpretation of the references to colour in this figure legend, the reader is referred to the web version of this article.)

totalizing approximately 820 m of ERT sections. The location of the abutment campaign sections is also shown in Fig. 2.

The sections from both campaigns were acquired parallel to the crest of the dam, with an approximate N-S orientation, and spacing between lines ranging from 10 to 15 m. The topography of the embankment campaign is flat, considering that the lines were acquired along the strike direction of the slope and did not reach the abutments. Diversely, the second campaign sections were acquired on the abutments where there were topography variations of up to 30 m.

The equipment used was the ABEM SAS4000 resistivimeter, with a 64-channel configuration. Before starting data acquisition, electrode array tests were performed using the Dipole-Dipole and Schlumberger arrays. The chosen array was the Dipole-Dipole, as it presented a considerably better signal-to-noise ratio, as well as an adequate depth of investigation versus lateral resolution relationship, confirming what has already been observed in published works (Dahlin and Zhou, 2004; Loke et al., 2013). The spacing between electrodes in both campaigns was 3 m. Fig. 3 illustrates the field operations on the dam.

The first acquisition campaign (embankment campaign), on the main embankment of the dam, was carried out during the dry season, and the second campaign (right abutment campaign), during the rainy season, as illustrated in Fig. 4.

3.2. Data processing

After the field survey, the field resistance measurements were reduced to apparent resistivity values. The data were then further processed and inverted using the Res2DInv software, which uses the smoothness-constrained Gauss-Newton least-squares inversion technique (Sasaki, 1992) to produce a 2D model of the subsurface from the apparent resistivity data, with resolution equivalent to half of the electrode spacing, or 1.5 m. From the model obtained, the apparent resistivity is calculated and compared with the actual measurements. The quality control routine consisted of the removal of clearly spurious points and filtering applied after a preliminary inversion of the data, where data with a large difference between the measured and calculated apparent resistivity were manually picked and discarded. As this is a non-linear problem, it is necessary to start with an initial model and iteratively perform corrections to this model, until a best-fit model (final model for interpretation) is obtained, based on the root-mean-squared error (RMS). In each iteration, the solution of the direct finite element problem is performed (calculation of theoretical resistivities) and, if the difference between the calculated and observed data does not satisfy the established convergence criterion of 5%, a correction vector is calculated (objective function) by least squares regularized inversion, to correct the resistivity model. For the inversion, the L1-norm was used, which seeks to find a model that minimizes data incompatibility absolute values.

Fig. 3. Photographic record of the ERT campaigns: (a) ABEM SAS4000 resistivimeter, (b)&(c) data acquisition on the crest, and (d) data acquisition on the slope of the embankment.

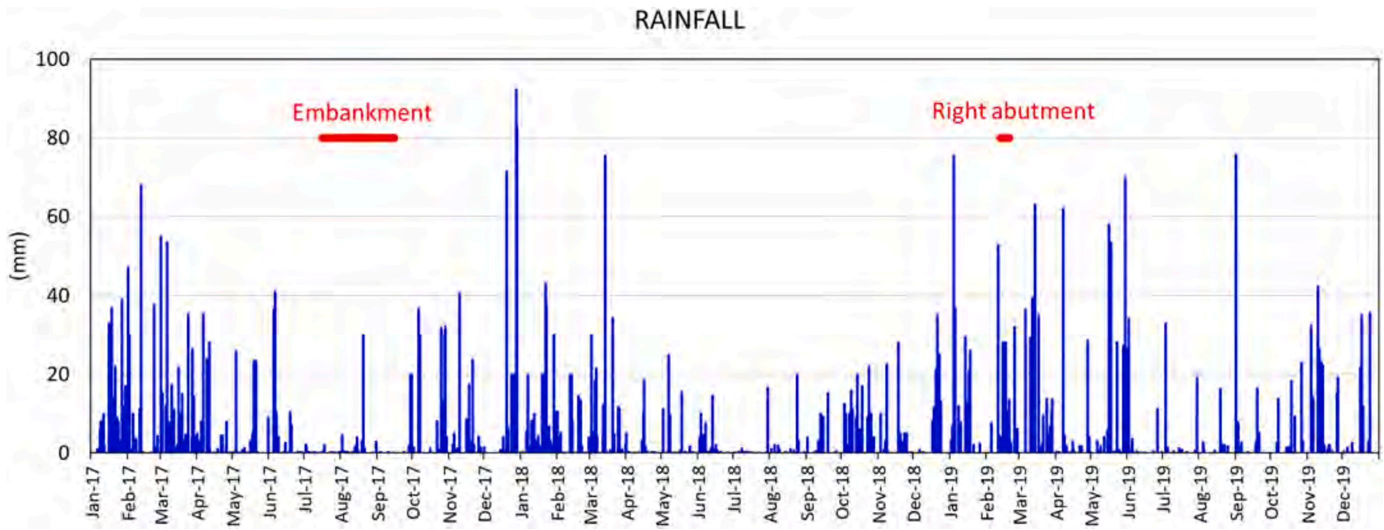

Fig. 4. Three years of rainfall measurements in the area of the dam (blue) and the period of each acquisition campaign (red). Source of rainfall data: DAEE – São Paulo State Department of Water and Electricity. (For interpretation of the references to colour in this figure legend, the reader is referred to the web version of this article.)

3.3. Data interpretation

After the data were processed and inverted, the 2D-resistivity sections were imported to a three-dimensional environment (*Leapfrog Geo*) to be merged with the structural features of the dam, as well as the available geotechnical information. After analyzing each ERT section, and comparing the anomalies ranges with the water level indicators measurements, three resistivity zones were defined for each campaign: Zones of low resistivity (LRZ), that might be correlated to regions of high humidity; zones of high resistivity (HRZ), that might be interpreted as dry zones; and regions with intermediate resistivity values (IRZ), located between these limits. Camarero and Moreira (2017) used a similar range classification in their study of an earth dam.

To integrate the described geophysical data with the geotechnical measurements from the dam, models in a three-dimensional environment were developed. The objective, in addition to a 3D visualization,

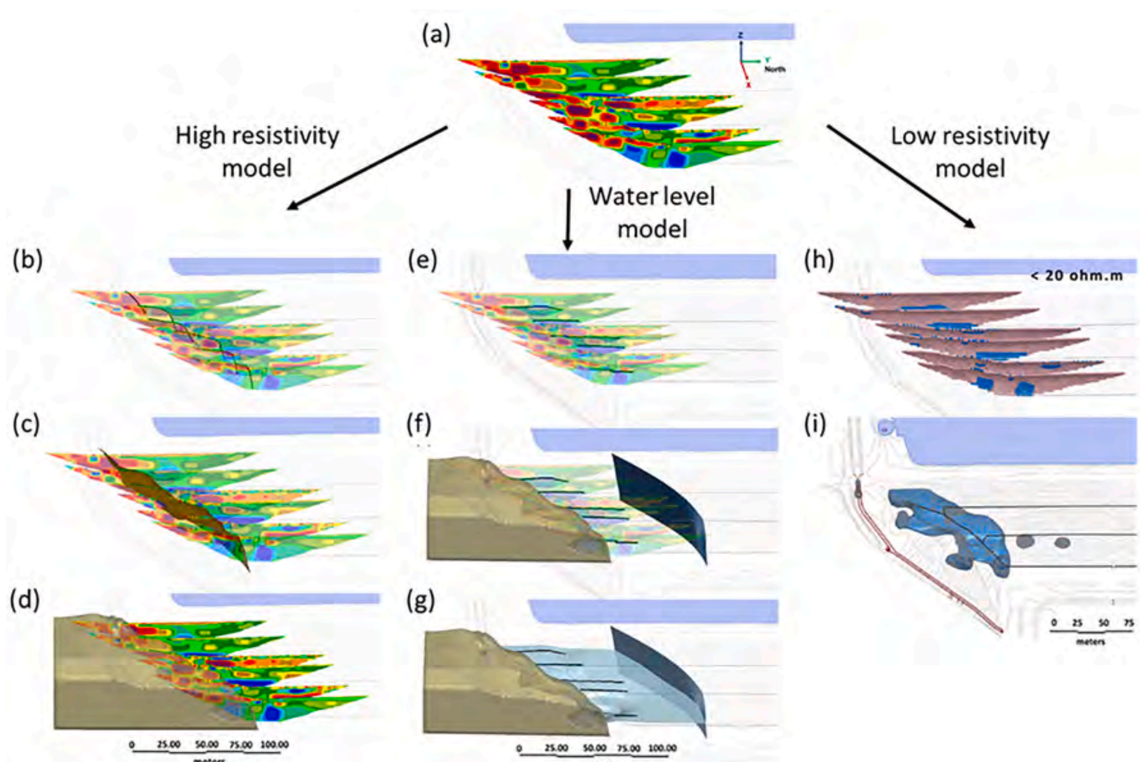

Fig. 5. Constructive methodology of the 3D model for the right abutment region. (a) 2D plots of the HRZs and LRZs distribution and their downstream continuity; (b) 2D delimitation of the HRZs in each section obtained; (c) 3D surface modeling from the delimitation lines; (d) development of a volume from the surface produced (e) delimitation of the LRZs; (f) definition of a boundary for the surface to be produced; (g) interpolation of the lines created to generate the surface associated with the water level; (h) classification of data with values below 20 Ω•m (blue); (i) 3D volume modeling from the LRZs that were delimited above the water level surface. (For interpretation of the references to colour in this figure legend, the reader is referred to the web version of this article.)

was to provide an integrated interpretation between both groups of data – geophysical and geotechnical – better representing the field geometry and preserving the spatial relationship of the dataset. The 3D modeling was executed using the software *Leapfrog Geo*, and among the main steps, some manual interpretation actions were required: the boundaries of the regions of low or high resistivity values (LRZ or HRZ) were vectorized for each geophysical section. From these vectors, it was possible to model surfaces and, later, volumes, using a volumetric spline interpolation to fit the data (Cowan et al., 2003), as illustrated in Fig. 5. A surface representing the water level was modeled from the nearby water level indicators (WLIs) and was merged with the surface created from the ERT data to validate and extend the 3D modeling. After that, a few regions that presented low resistivity values, even above the inferred water level, were modeled and these volumes were included in the 3D model.

Fig. 5 details the construction methodology of the high resistivity model (abutment natural terrain), water level model, and low resistivity (above water level) model, consisting, basically of the following steps:

A. High Resistivity Zone (HRZ) model:

- Insertion of acquired geophysical sections in the modeling software (Fig. 5(a))
- Manual digitalization of the boundaries of the resistive portion (HRZ) in each ERT section (Fig. 5 (b));
- Surface interpolation from the vectorized boundaries (Fig. 5 (c));
- Construction of the 3D volume associated with the right abutment combining the interpolated surface with the local topography (Fig. 5 (d)).

B. Water Table Model:

- Insertion of acquired geophysical sections in the modeling software (Fig. 5(a))
- Manual digitalization of the top boundaries of the continuous conductive horizon (LRZ) in each ERT section (Fig. 5 (e));
- Creation of a boundary (wall) to limit the surface to the ends of the ERT sections (Fig. 5(f));
- Surface interpolation from the vectorized boundaries and implicit modeling extrapolation of the water table, limited to the “wall” (Fig. 5 (g)).

C. Low Resistivity Zone (LRZ) model

- Insertion of acquired geophysical sections in the modeling software (Fig. 5(a))
- Selection of the LRZ values equal to and below 20 Ω•m (Fig. 5 (h));
- Implicit 3D modeling of the volume associated with the LRZ possibly representing humid zones (Fig. 5(i));

4. Results

4.1. Embankment campaign

The ERT data from the embankment campaign were processed, inverted, and displayed as 2D sections that were compared to the water level indicator's data (WLIs) so that the low resistivity range corresponding to the presence of water could be identified, as illustrated in Fig. 6. Values below 84 Ω•m were associated with higher humidity contents. The interpretation performed on the 2D sections was consistent in differentiating high and low resistivity anomalies with a strong correlation to the WLIs measurements. Three main resistivity domains were observed in the electric resistivity sections: LRZ (Low Resistivity Zone), with values below 84 Ω•m; IRZ (Intermediate Resistivity Zone), with values between 84 and 500 Ω•m, and HRZ (High Resistivity Zone), corresponding to values above 500 Ω•m.

From the data already processed in the Res2DInv software, a text file was generated, containing the values of the spatial coordinates and resistivity values for each point of the inverted sections (Figs. 7(a)& (b)). Through this information, electrical data underwent further processing - with the assistance of interpolation tools - resulting in a continuous three-dimensional model of electrical resistivity along the embankment.

The analysis focused on the region around the right abutment, partially covered in the embankment campaign, mapped several low resistivity zones, forming ellipsoidal conductive anomalies, which extended to the region of the rocky abutment, as illustrated in Figs. 7(c)

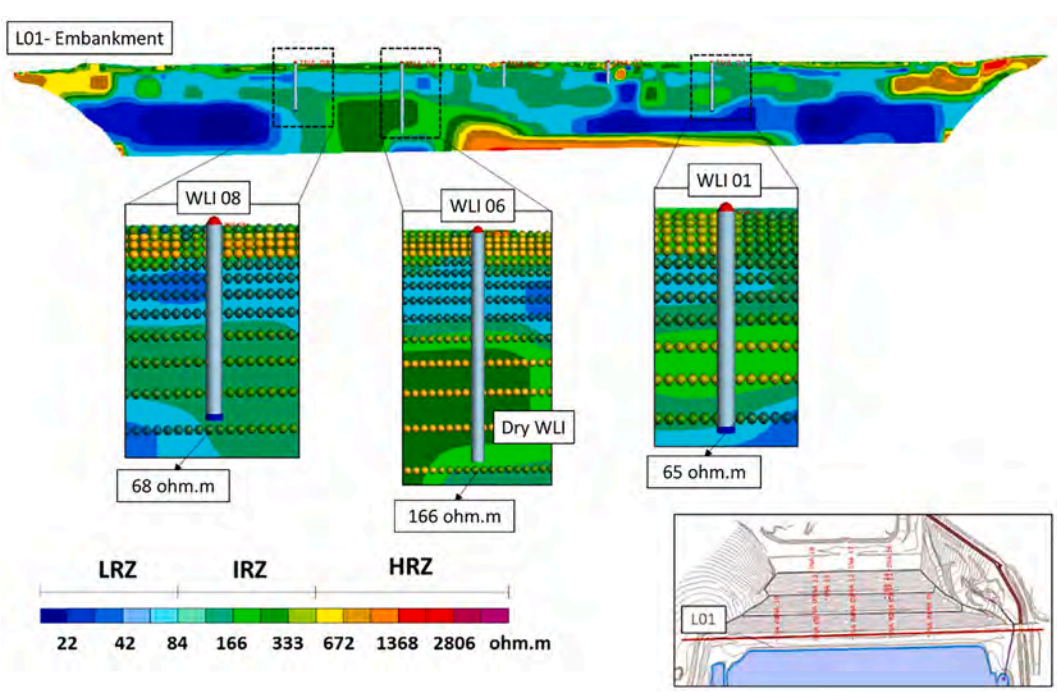

Fig. 6. Comparison of an ERT section on the crest of the dam and the water level indicators' (WLI) water level.

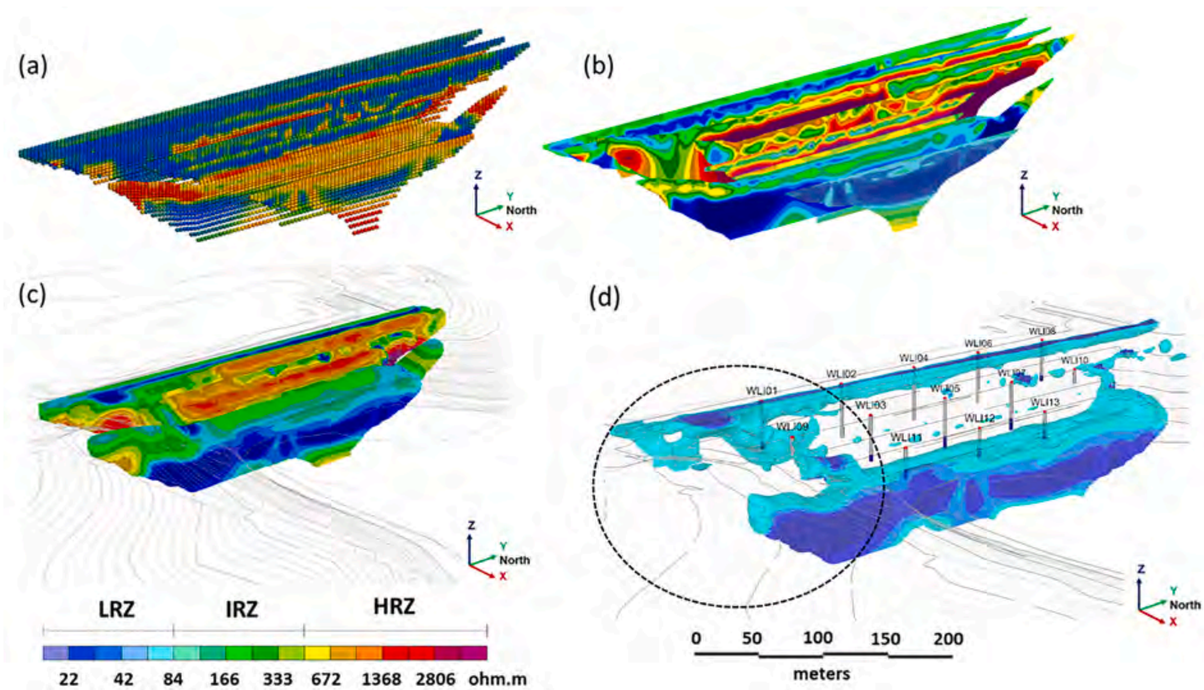

Fig. 7. Electrical resistivity data at the dam, referring to the embankment campaign (L01 to L08). (a) Resistivity points; (b) Interpolated sections; (c) Resistivity three-dimensional model, generated from sections L01 to L08; (d) Low resistivity zones (<84 Ω•m), with emphasis on ellipsoidal anomalies in the region of the right abutment.

& 7(d), raising the possibility that they were conditioned by the presence of zones with high moisture content, marked with a dotted circle in Fig. 7(d). The main result of the embankment campaign analysis using the ERT operational workflow was the detection of many low resistivity zones at the right abutment defining a "zone of attention" that required further characterization.

The classification of the main resistivity zones allowed the modeling of the water table, using the geometry of the low resistivity zones and WLI measurements. The continuity of the LRZs was especially important where there are no WLIs installed. Fig. 8 illustrates the construction of the surface of the water table, through the interpolation of the WLI measurements and the top limits of the LRZs.

After the analysis of the embankment campaign data, the hypothesis was raised that there was some moisture in the region of the right

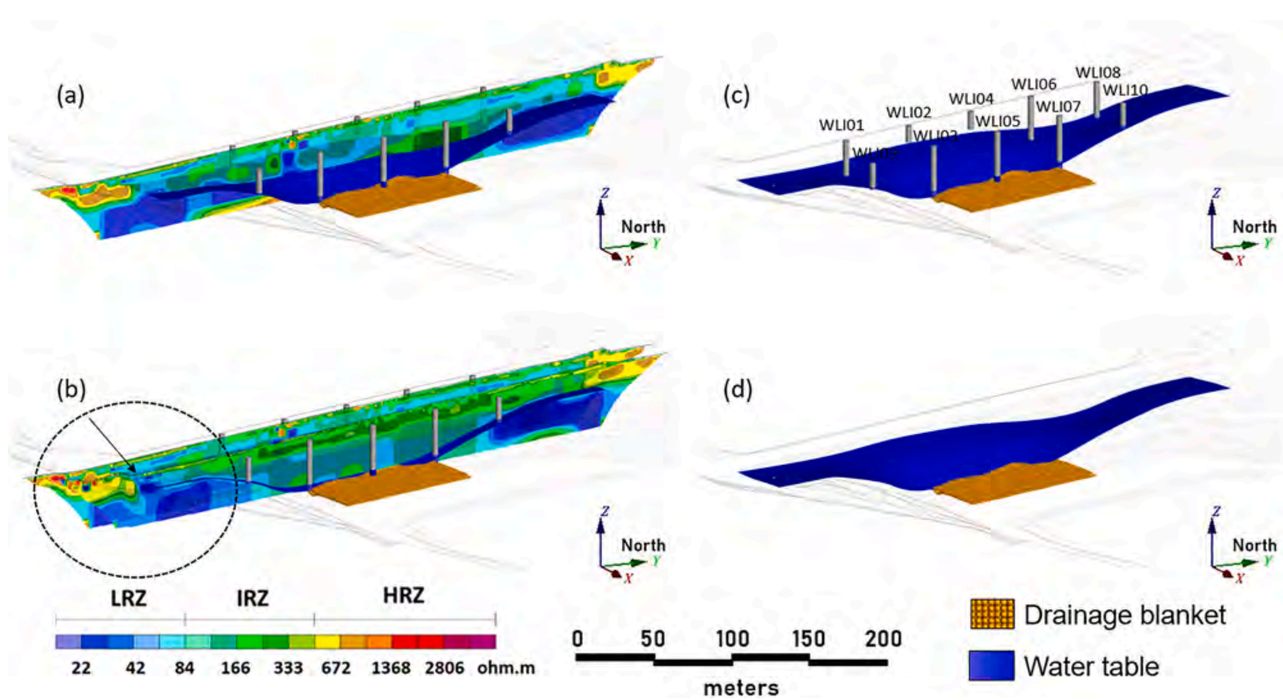

Fig. 8. The strong correlation between WLI measurements, the interpreted water level, and the low resistivity zones (LRZ) can be observed: (a) section L01 compared to the WLI, drainage blanket, and interpreted water table; (b) L01 (back) and L02 (front) compared to the WLIs, drainage blanket, and interpreted water table; (c) WLIs, drainage blanket, and interpreted water table; (d) the drainage blanket, and the complete surface of the interpreted water table.

abutment (above the water level surface), whose origin was not elucidated at the time, indicated by the arrow in Fig. 8(b). As a result, a set of new sections was planned and acquired in the region (abutment campaign), to gain a better understanding of the disposition of these conductive zones, as well as their conditioning factors.

4.2. Right abutment campaign

The field campaign on the right abutment consisted of the acquisition of six ERT sections parallel to the embankment campaign ones, totalizing 820 m of profiles. The electrical resistivity sections obtained reached from 25 to 33 m in depth, being consistent with the embankment campaign in the differentiation of anomalies from high to low resistivity (Fig. 9).

Three main resistivity domains were observed in the electric resistivity sections of the right abutment: LRZ (Low Resistivity Zone), with values below 20.0 Ω•m; IRZ (Intermediate Resistivity Zone), with values between 20.0 and 127.0 Ω•m and HRZ (High Resistivity Zone), corresponding to values above 127.0 Ω•m.

Comparing these sections with the ones from the previous campaign, it was noted that the range of resistivity values was narrower. A reasonable explanation for this fact is the rainy season in which they were acquired since excess moisture in the substrate causes an increase in the conductivity of the materials (Dentith and Mudge, 2014; Braga, 2016).

The distribution of geophysical signatures along the collected sections generally followed the same pattern: discontinuous HRZs predominate, interspersed with IRZs, on the horizon closer to the surface. At greater depth, it is possible to observe that all sections have well-marked HRZs restricted to the region of the right abutment. These zones gradually change to IRZs in the embankment region. At basal levels, LRZs predominate and show a degree of lateral continuity along the sections. Conductive anomalies also occur immersed in HRZs at the beginning of the sections, although they are more localized. Fig. 10 illustrates the features described above.

4.2.1. Right abutment data modeling

The region of the right abutment demanded more detailed models because of its structural complexity due to the contact *between the natural terrain and the embankment materials*, with different textures and porosities, where there are no geotechnical instruments installed. The natural terrain in this area is composed of sandy soils overlying saprolite and rock, and supports a large spillway, access roads, and other facilities. The results of both campaigns, showing many small LRZs unrelated to the water table (Figs. 7(d) & 8 (b)) lead to the inference, in depth, of the boundary between natural terrain and embankment, to detail the water table inside the abutment, and to refine the model of the humid areas.

4.2.1.1. High resistivity model. As seen in Fig. 11, the geophysical

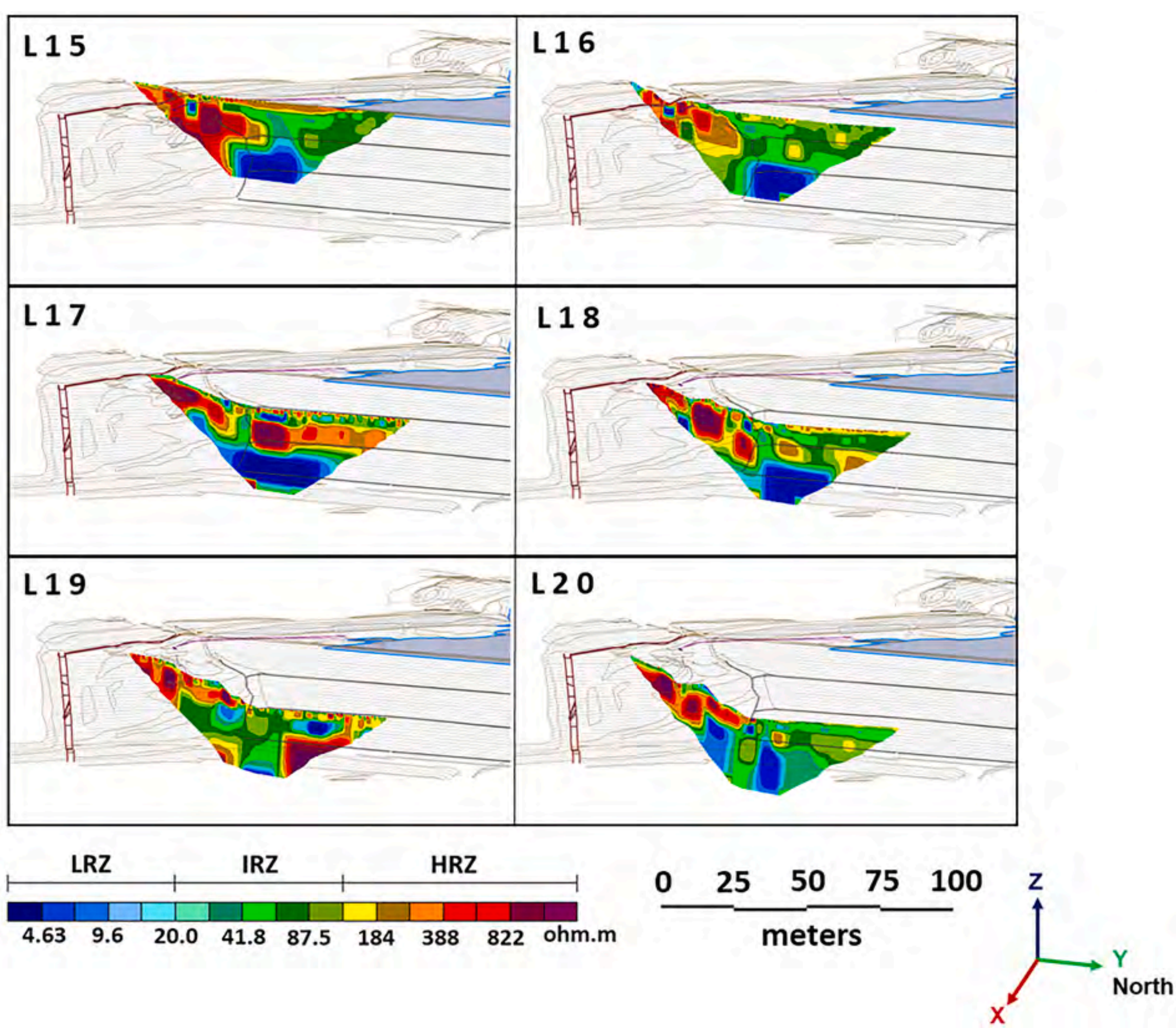

Fig. 9. Electrical resistivity sections, for lines L15 to L20 (from top left to bottom right), obtained at the right abutment of the dam.

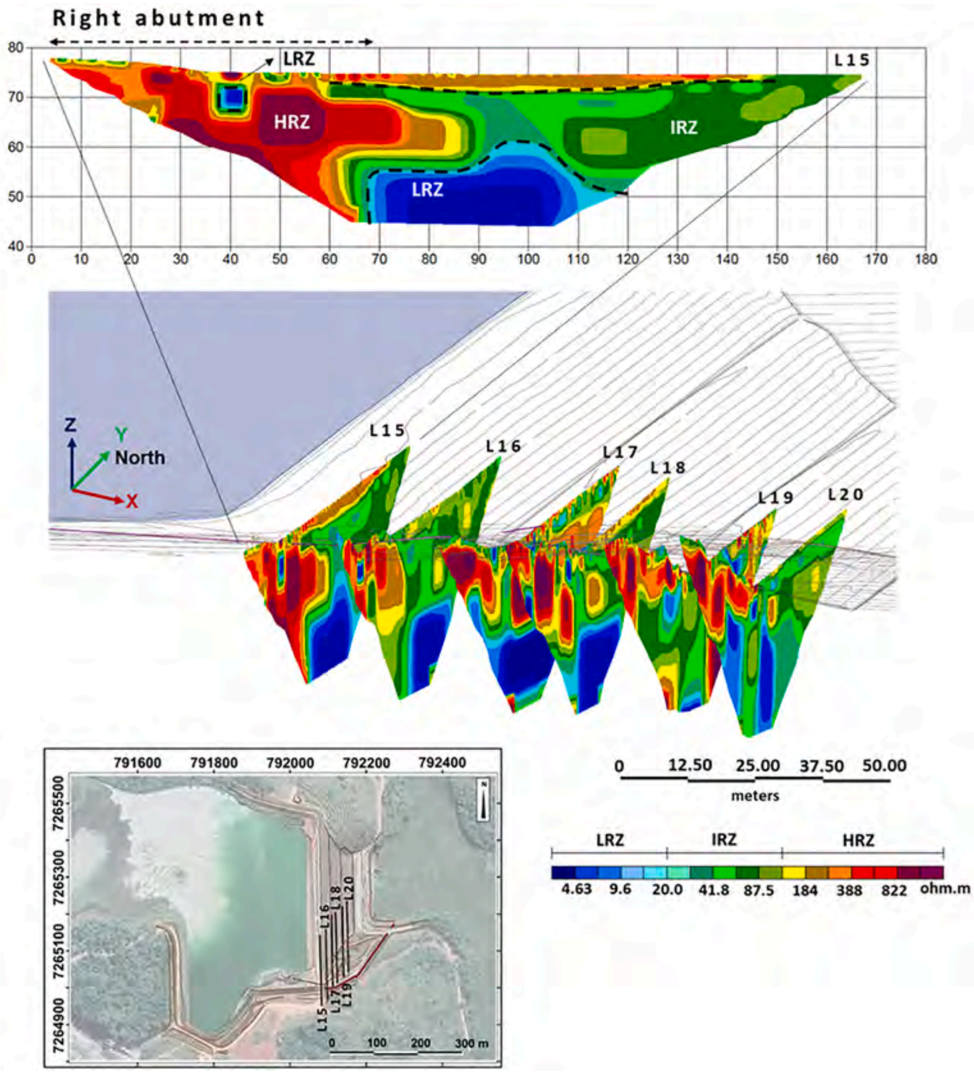

Fig. 10. Example of the main domains observed throughout the electrical resistivity survey (L15), and below, the disposition of the geophysical sections surveyed in the region of the right abutment of the dam.

sections mostly presented HRZ in their beginning, which, spatially, coincided with the region of the right abutment (natural terrain). As a result, the high resistivity values (> 127 Ω•m) could be associated with the materials present in the terrain, which were: colluvial soil with clayey texture, underlaid by residual Jacupiranguito soil, with textures ranging from clayey-silty to silty-sandy, and fragments of altered rock.

From the correlations performed for the interpretation of the right abutment, the contour of the zones, present in the geophysical sections, which presented high resistivity values, was vectorized. With this, it was possible to model a surface and, later, a volume, which was representative of the natural terrain (Fig. 12).

4.2.1.2. Water level model. Along all sections, it was possible to observe the presence of LRZs, arranged continuously, in depth, whose values were lower than 20 Ω•m. These domains, due to the low resistivity values and continuous horizontal disposition, were associated with the presence of regions with high water content. Because of their location and continuous arrangement, they were correlated with the water level of the structure (Fig. 13).

Due to the distribution of the water level indicators (WLI) on the dam, it was not possible to carry out a direct correlation in the region of the geophysical sections with these instruments. However, when projecting the interpreted water level, from the geophysical survey to the closest WLIs, a similarity was observed between the water level, obtained from geophysics, with the level observed in the instrument, corroborating the analyzes carried out from geophysical data, as indicated by the dashed lines in Fig. 13.

With the validation of the parameters used to interpret the sections, the contacts were considered delimiters of the water level of the structure and were also vectorized, with the purpose of modeling it for the region.

It should be noted that the surface boundaries were extended beyond the region in which the geophysical data were acquired, based on the correlations illustrated in Fig. 13.

Fig. 14 presents a three-dimensional representation of the water level surface in the region of the right abutment validated by the extrapolated water level indicators measurements.

4.2.1.3. Low resistivity zones model. For the region of the geophysical survey, the characteristic resistivity range (values below 20 Ω•m) was defined for areas with high water content, associated with the structure's water level, and corroborated by employing the instrumentation of the dam (in this case, the WLIs).

After that, numerical limits were set to the three-dimensional model of the resistivity data, aiming at individualizing the regions that presented values lower than 20 Ω•m above the previously modeled water

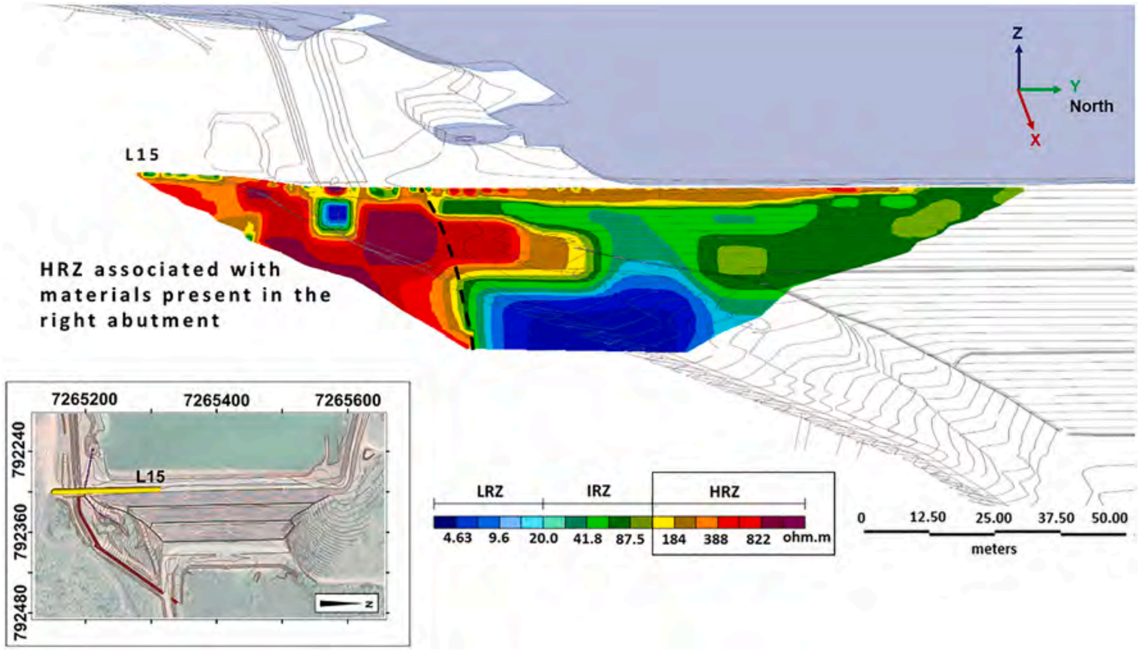

Fig. 11. Delimitation of the high resistivity zones, in L15, interpreted as related to the materials present in the right abutment (natural terrain).

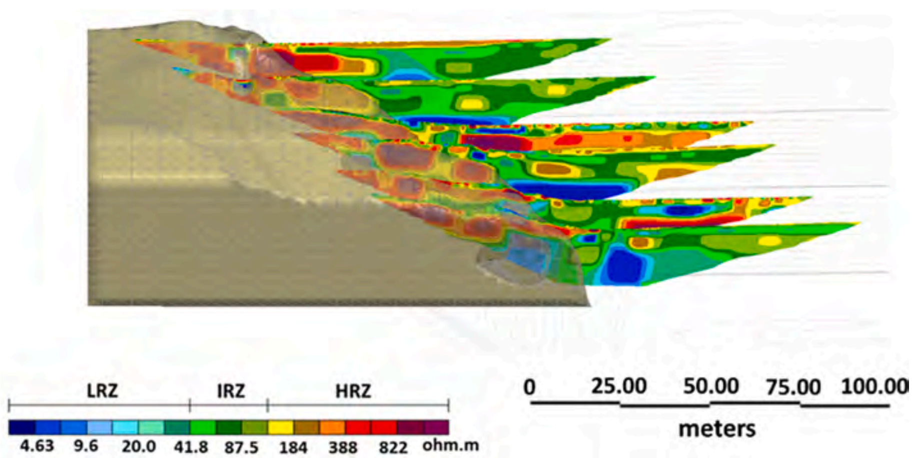

Fig. 12. 3D volume model of the natural terrain in the right abutment region.

level, highlighting regions that represent possible humidity spots inside the structure.

Fig. 15 displays all the models of the right abutment: high resistivity model, water level surface, and lower resistivity zones emphasized in blue.

Once the volumes associated with conductive zones (< 20 Ω•m) were modeled it was possible to spatially assess the insertion of these zones in the context of the right abutment and embankment, correlating them with some structural features of the dam, as well as its water level (Fig. 15). The LRZ model geometry suggests a contribution of moisture from the natural terrain, composed predominantly of sandy soils, saprolite and/or rock, towards the dam's embankment.

LRZs, still interpreted as zones with high water content, were also observed near the surface. It was observed that some were located and oriented towards the spillway and water drainage channels, as shown in Fig. 16.

4.3. *Operational workflow*

After joining all the models generated using the ERT dataset and comparing them with the operational information from the main structures, we propose a risk assessment analysis aiming to support the decision-making about the dam management as defined in the ERT operational workflow. This workflow results from the discussion between different areas such as geotechnics, civil engineering, dam operations, and top management, and represents a way to incorporate geophysical results into the risk management of the dam. The processes described above culminated in the ERT operational workflow that is represented in Fig. 17, which details the main steps of the ERT operational workflow, developed for this work, aiming to incorporate ERT surveys in the inspection routine of the dam. This incorporation can become an important tool to guarantee, under specific geologic conditions, one more variable for characterizing the humidity distribution inside these structures and supporting the risk assessment of many operational decisions.

Once the targets are modeled in a 3D environment, the resistivity results are compared with the geotechnical instrumentation dataset to confirm that the mapped 3D geobodies actually correlate with moisture zones representing zones of attention, other steps are still needed to support a better management decision. Table 1 below lists the criteria to

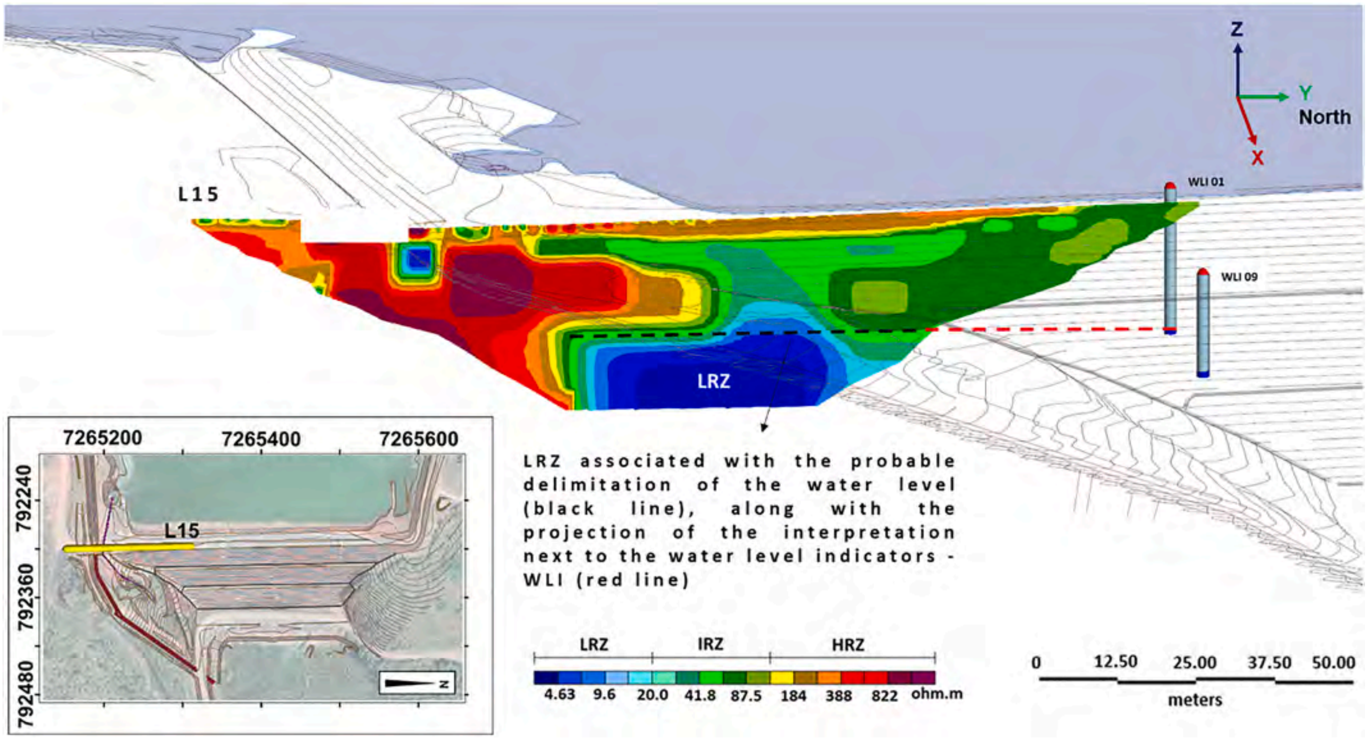

Fig. 13. Delimitation of an LRZ, on section L15, interpreted as related to the water level, with its projection, in red dashed line, corroborated by local water level indicators. (For interpretation of the references to colour in this figure legend, the reader is referred to the web version of this article.)

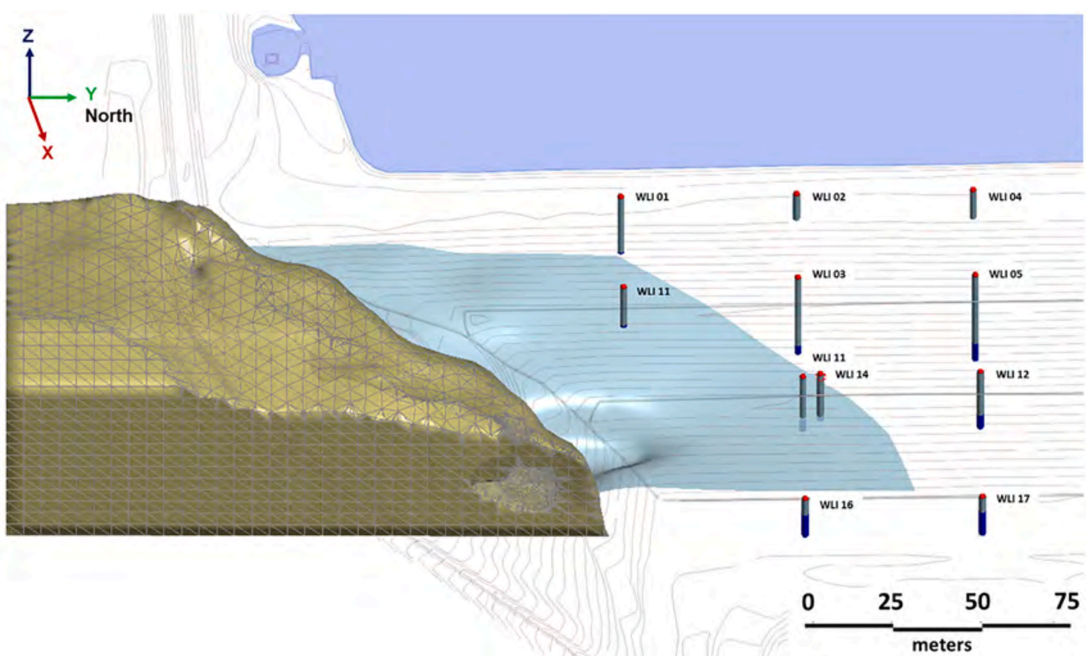

Fig. 14. Visualization, in perspective, of the modeled water surface, validated by the records obtained from the water level indicators (WLI).

proceed with the risk analysis and take the decision about follow-up surveys and/or field intervention.

Despite having eight criteria to perform the risk analysis, once the two top (geophysical) criteria in the table are present, just one more from the list is enough to characterize that the mapped 3D geobodies have a high probability to represent high water content zones and need intervention under the whole risk management process.

Table 2 shows the results of the risk assessment spreadsheet properly filled considering the specific case of this work.

Criterion 1 of the Risk Criteria Table was met in the two campaigns, as some low conductivity anomalies are located in similar positions along the sections and extend well beyond the resolution of the surveys (1.5 m), as well as criterion 2, because many of the anomalies can be seen in several sections. Criterion 3 was met in both campaigns, despite the absence of WLIs in the right abutment, because the water table surface was extended using implicit modeling using the nearest

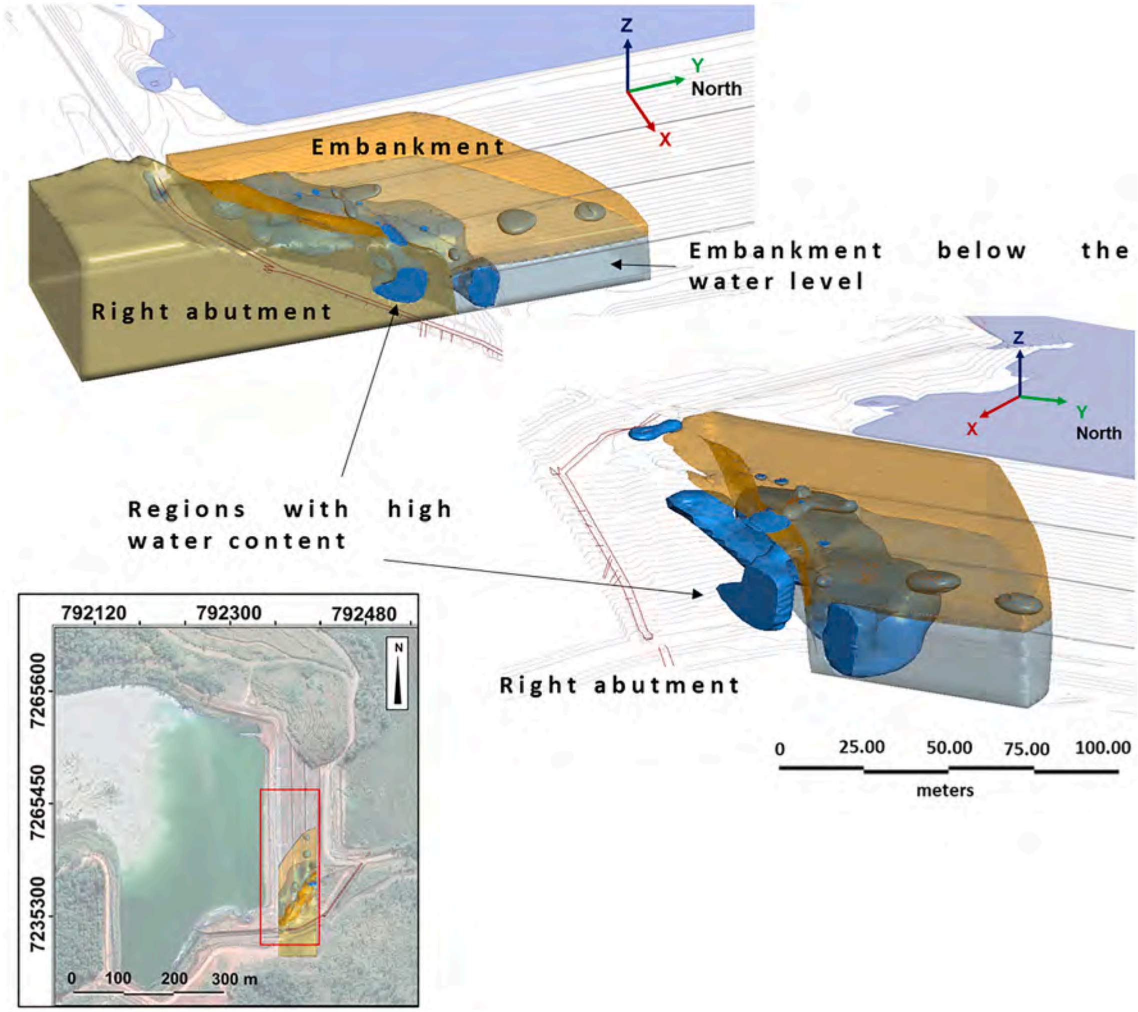

Fig. 15. Distribution of the most conductive zones modeled (in blue), in the region of the right abutment, along with the other components from the created model: in brown, the right abutment; in orange, the region of the embankment, above the water level; and in light blue, the region of the embankment, below the water level. (For interpretation of the references to colour in this figure legend, the reader is referred to the web version of this article.)

instruments. As there aren't any instruments in the right abutment, criterion 4 couldn't be applied. Criterion 5 was met because some very well-defined anomalies could be seen directly below the spillway, indicating that there is humidity related to this structure. Criterion 6 is met using the 3D model, whose shape suggests that the humidity is migrating from the natural terrain of the abutment to the embankment. Criteria 7 and 8 were not met because, to our knowledge, there were no geotechnical interventions that could affect our results, and we didn't have access to data from any other geophysical campaigns executed during the period of this study. In summary, as the two first criteria and three additional ones from the table were met, there is a need to proceed with the investigations and possibly do some intervention in the dam.

5. Discussion

The interpretation of the results identified low resistivity anomalies that, considering some constraints and assumptions, may represent a point of attention for the dam's safety. The simple existence of low resistivity anomalies inside the structures (embankment, abutments) indicates the need for further investigations. Any seepage out of the drain structure is a concern for the operational management of the dam, but the link with possible causes is beyond the capacity of geophysical dataset insights.

Furthermore, the direct checking in depth (drilling, sampling) that low resistivity anomalies represent humid areas inside the structure (above the water table) can bring a higher risk for the dam safety than multiple ERT surveys correlated with the dam's routine operations. The interpretation of the time-lapse ERT results may answer questions like: Do the anomalies increase in the rainy season? Do the anomalies change during spigot disposal? These are key questions for defining the correlation between low resistivity anomalies versus humidity spots in depth. If the answer to any of the questions is yes, it is demonstrated that the low resistivity anomalies are important variables to monitor humid areas inside the structures of tailings dams. At this point, we can say that directly checking anomalies in depth without increasing the risk for the dam operation is a technological challenge. In summary, the risk of direct intervention can be higher than monitoring using indirect methods constrained by dam instruments.

The time-lapse approach was barely used in this study, as there is only a small overlap between the two acquisition campaigns, enough to address the low resistivity anomalies expansion in the region of the right abutment. The ideal approach would be permanent monitoring, or at least a campaign per season, ensuring that the sections overlap as much as possible and the electrodes are installed in the same place and have the same coupling to the terrain from one campaign to the other. However, repeatability is not always possible since tailings dams are living structures subject to raisings or reinforcements, or other interventions that change their geometry.

The option to execute the survey acquisition just in the strike direction (parallel to the crest) represents an operational optimization

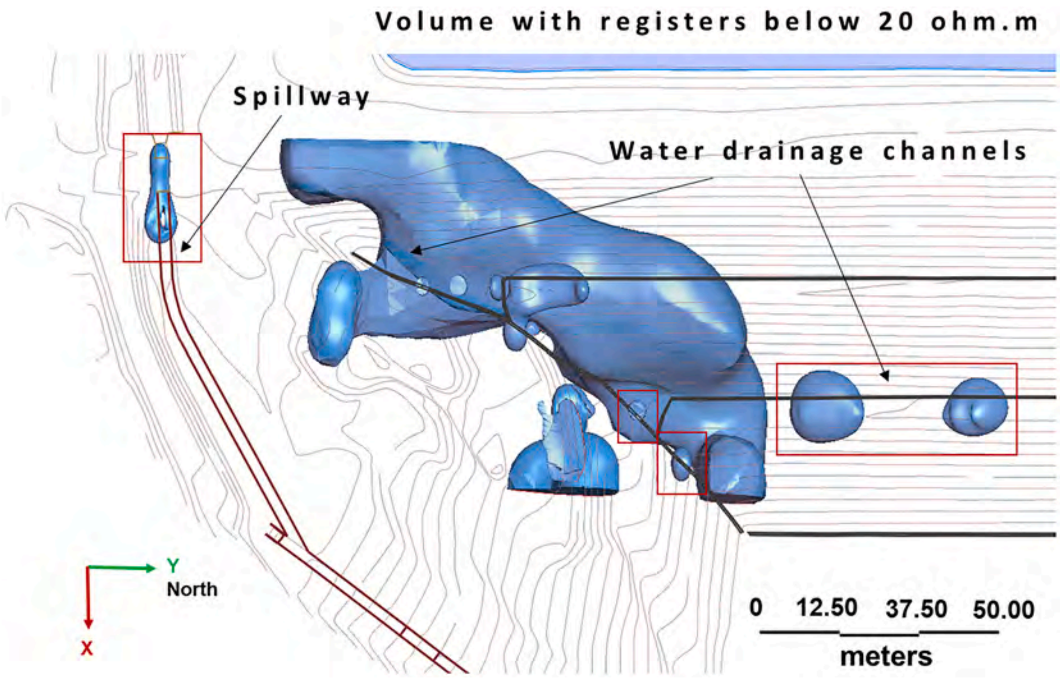

Fig. 16. Regions of higher conductivity inserted in the context of the right abutment interpreted and associated with the spillway and water drainage channels of the dam.

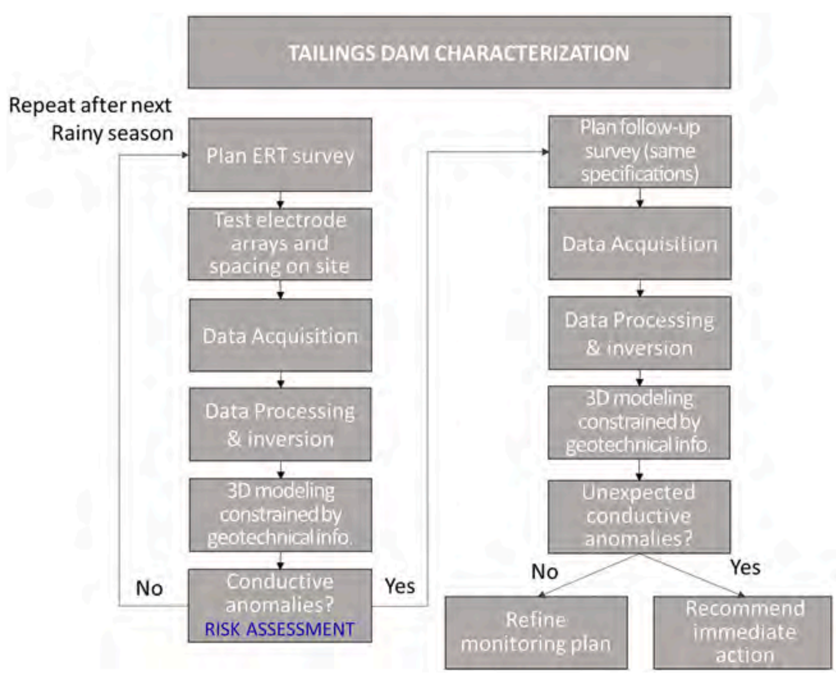

Fig. 17. ERT operational workflow demonstrating generic steps for tailings dam characterization.

since the electrodes are placed mostly at the same level and the resulting sections cross the probable downward flow path of any seepage. The 2D acquisition geometry represents a limitation since the ideal array for the nature of the seepage phenomenon would be a 3D one. All these limitations in the acquisition are mostly due to budget constraints. The proposed operational workflow (Fig. 17), especially in the modeling step, attempts to mitigate these limitations by using implicit modeling (Leapfrog Geo) to interpolate anomalies between sections.

The operational workflow still requires manual interpretation within the process and different interpreters may pick up different low resistivity zones generating different humid zones. The instruments readings are also manual, therefore subject to mistakes, and the frequency of readings might not coincide with the changes in the water level. The automation of the instruments (IoT) may lead to new insights about the behavior of the water inside the structures.

Dams composed of other types of tailings may present different resistivity/conductivity behaviors to map humid areas or seepage, but this does not make the ERT method unfeasible, it just complicates the interpretation. Measuring the efficiency of the proposed operational workflow or any other geophysical criteria to early identify problems to

Table 1
Proposed risk criteria spreadsheet.

	Risk criteria	Base survey	Follow-up survey
1	*Anomaly geometry consistency (shape, extension, location along the section)?*		
2	*Continuity (is the anomaly present in 2 or more sections)?*		
3	Is the anomaly correlating with any monitoring instruments (yes, barely, no)?		
4	Is the anomaly correlating with 2 types of instruments (yes, barely, no)?		
5	Is the anomaly correlating with field observations (yes, barely, no)?		
6	Is the anomaly geometry indicative of flow direction (yes, barely, no)?		
7	Was there any intervention that might impact the anomaly generation (spigot disposal - construction)		
8	Another geophysical method indicating humidity and/or flow?		

Table 2
Risk criteria spreadsheet filled out for the surveyed dam.

	Risk criteria	Base survey	Follow-up survey
1	*Anomaly geometry consistency (shape, extension, location along the section)?*	x	x
2	*Continuity (is the anomaly present in 2 or more sections)?*	x	x
3	Is the anomaly correlating with any monitoring instruments (yes, barely, no)?	x	x
4	Is the anomaly correlating with 2 types of instruments (yes, barely, no)?		
5	Is the anomaly correlating with field observations (yes, barely, no)?	x	x
6	Is the anomaly geometry indicative of flow direction (yes, barely, no)?	x	x
7	Was there any intervention that might impact the anomaly generation (spigot disposal - construction)		
8	Another geophysical method indicating humidity and/or flow?		

avoid dam failure is a hard task since the risk management of dams has improved and the management has to act early to prevent any new disasters and also because many tailings dams are being decommissioned or decharacterized in Brazil (e.g. Massignan and Sánchez, 2022). The proof of effectiveness itself would depend on a negative that is unfeasible because no one will test operational interventions to demonstrate the effectiveness of a methodology. The proposed workflow can be incorporated into the monitoring system of any tailings dam, to meet the requirements of the Global Industry Standard on Tailings Management (While we acknowledge that any tailings dam is a hazard, we believe that ERT data interpretation can help to reduce the risk of dam failure. We kept the word "risk" in the title, as suggested by reviewer 3, and went over all the other occurrences in the text. The first paragraph of the abstract discusses the operational safety of the dam. We changed several parts of the abstract to make it clear what the ERT's purpose is. The term 'risk management' rather than 'hazard management' is used in the Global Industry Standard on Tailings Management (United Nations Environment Programme, 2020), which recommends that the management of a tailings facility implements an integrated monitoring system that incorporates the available technologies recorded at appropriate frequencies and to confirm through the lifecycle of the structure that they remain effective to manage risk.

Faced with several uncertainties, it is better to image than to continue without any information about what happens between the water level indicators and other geotechnical instruments. Although the ERT method and data interpretation demonstrate procedural weaknesses and that every data series is valid for an undisturbed condition of the environment, the value of the method is very clear in that it allows the interpreter to investigate what is going on between the direct monitoring instruments. In the case of reinforcement works or raisings, it is expected that a new series of surveys will define different water distributions.

6. Conclusions

Low resistivity zones, defined as zones with values lower than 84 Ω•m in the embankment campaign a5nd lower than 20 Ω•m in the right abutment campaign, were related to regions with high moisture content. The disposition of these zones, due to the lateral and in depth continuity, highlighted the geometry of the water level. This feature, modeled from geophysical data, at depths ranging from 30 m below ground in the center of the embankment, to 15 m when it gets closer to the abutments, showed consistency with the data presented by conventional instrumentation, in this case, water level indicators, so it was possible to indicate that the ERT operational workflow achieved a broad characterization of the dam, inferring high water content zones, and the water level surface based on a very simple methodology.

The anomaly distribution of the low resistivity volumes mapped in the right abutment, extending from the embankment at depths ranging from 10 m deep to the water table, indicates a possible contribution of moisture from the natural terrain towards the embankment. In addition, spatial coherence was noted between the conductive zones, closer to the surface, at depths of <5 m below ground, with water drainage channels and the spillway. The geometry of these anomalies is well mapped with the electrode spacing of 3 m and the obtained resolution of 1.5 m.

The ERT results can spatially complement the traditional methods of monitoring dams, provide a broad view of the moisture distribution in the structure and demonstrate its hydraulic behavior in regions that are not covered by the installed instrumentation.

The application of ERT in mapping humid zones was validated and we recommend that it becomes an operational tool to be incorporated into the routine risk management of any tailings dam. For that purpose, an operational workflow and a risk assessment spreadsheet were proposed.

Some guidelines can be extracted from this experience. In a time-lapse analysis of ERT datasets, the follow-up survey should repeat as much as possible the acquisition specifications from the base survey. Dam instruments are great constraints to ERT interpretation and modeling of the targets of the survey. Comparing the results from the base survey, executed in the dry season, and the follow-up survey, acquired in the rainy season in the region of the right abutment we suggest follow-up surveys shall be executed at the end of the rainy season and compared with previous surveys, if available.

CRediT authorship contribution statement

Lorena Andrade Oliveira: Writing – original draft, Conceptualization, Methodology, Software. **Marco Antonio Braga:** Conceptualization, Methodology, Validation, Resources, Project administration. **Guilherme Prosdocimi:** Formal analysis, Software, Data curation. **Alan de Souza Cunha:** Writing – review & editing, Conceptualization, Methodology, Software. **Leonardo Santana:** Validation, Resources. **Filipa da Gama:** Writing – review & editing, Conceptualization, Methodology, Software.

Declaration of Competing Interest

- The authors have no relevant financial or non-financial interests to disclose.
- The authors have no conflicts of interest to declare that are relevant to the content of this article.

- All authors certify that they have no affiliations with or involvement in any organization or entity with any financial interest or non-financial interest in the subject matter or materials discussed in this manuscript.
- The authors have no financial or proprietary interests in any material discussed in this article.

Data availability

The authors do not have permission to share data.

Acknowledgements

We would like to thank Mosaic Fertilizantes for funding this research and allowing access to the B1 Dam data. We are also very grateful to the reviewers for taking the time and effort necessary to review the manuscript. We sincerely appreciate all valuable comments and suggestions, which were of great help to improve the quality of the manuscript.

References

Albuquerque, R., et al., 2019. Caracterização de barragens de rejeito usando Geofísica Rasa: Aplicação da Barragem B1 de Cajati, São Paulo. Anuário do Instituto de Geociências – UFRJ 42 (1), 567–579.

Al-Fares, W., 2014. Application of electrical resistivity tomography technique for characterizing leakage problem in Abu Baara earth dam, Syria. Int. J. Geophys. 2014, 1–10.

Azam, S., Li, Q., 2010. Tailings dam failures: A review of the last one hundred years. Waste geotechnics. Geotech. News 28, 50–54.

Bogoslovsky, V.A., Ogilvy, A.A., 1970. Application of geophysical methods for studying the technical status of earth dams. Geophys. Prospect. 18, 758–773.

Braga, A.C.O., 2016. Métodos Geoelétricos em Hidrogeologia. Oficinas de Textos, São Paulo, p. 160.

Breitenbach, A.J., 2010. Overview: tailings disposal and dam construction practices in the 21st century. In: Tailings and Mine Waste 2010: Proceedings of the 14th International Conference on Tailings and Mine Waste, Vail, Colorado, USA, 17–20 October 2010, pp. 49–57.

Butler, D.K., 1984. Geophysical methods for seepage detection, mapping and monitoring. In: 54th SEG Meeting, 1984, Atlanta, Expanded Abstracts, pp. 157–160.

Camarero, P.L., Moreira, C.A., 2017. Geophysical investigation of earth dam using the electrical tomography resistivity technique. REM-Int. Eng. J. 70, 47–52.

Cowan, E.J., et al., 2003. Practical Implicit Geological Modelling, 5th International Mining Geology Conference Proceedings, AusIMM Publication Series 8/2003, pp. 89–99.

Dahlin, T., Zhou, B., 2004. A numerical comparison of 2D resistivity imaging with 10 electrode arrays. Geophys. Prospect. 52, 379–398.

De Oliveira Neves, A.C., et al., 2016. Neglect of ecosystems services by mining, and the worst environmental disaster in Brazil. Natureza & Conservação 14 (1), 24–27.

Dentith, M., Mudge, S.T., 2014. Geophysics for the Mineral Exploration Geoscientist. Cambridge University Press, Cambridge, p. 438.

Derby, O.A., 1891. The magnetite ore districts of Jacupiranga and Ipanema, São Paulo, Brazil. Am. J. Sci. 141 (3), 311–321.

Fata, Y.A., et al., 2021. Seepage patterns in an earth-rock fill dam evaluation using electrical resistivity tomography (ERT) method. In: IOP Conference Series: Earth and Environmental Science. IOP Publishing, p. 012090.

Fell, R., et al., 2015. Geotechnical Engineering of Dams, 2nd edition. CRC press, London, p. 1374.

Guireli Netto, L., et al., 2019. 3D geophysical investigation from the methods of eletroresistivity, self-potential and seismic refraction in an earth dam. In: Near Surface Geoscience Conference & Exhibition, 2019, The Hague, Netherlands. 25th European Meeting of Environmental and Engineering Geophysics, Held at Near Surface Geoscience Conference and Exhibition 2019, NSG 2019. Available at. http://hdl.handle.net/11449/221513.

Guireli Netto, L., et al., 2020. A utilização de métodos geofísicos na investigação de uma pequena barragem de terra. Boletim SBGf 112, 12–15.

HIMI, M., et al., 2016. Using the resistivity method for leakage detection at Sant Llorenç de Montgai Embankment (Lleida, NE Spain). In: Near Surface Geoscience 2016-22nd European Meeting of Environmental and Engineering Geophysics. European Association of Geoscientists & Engineers cp-495-00024.

Johansson, S., Dahlin, T., 1996. Seepage monitoring in an earth embankment dam by repeated resistivity measurements. Eur. J. Environ. Eng. Geophys. 1 (3), 229–247.

Loke, M.H., Chambers, J.E., Rucker, D.F., Kuras, O., Wilkinson, P.B., 2013. Recent developments in the direct-current geoelectrical imaging method. J. Appl. Geophys. 95, 135–156.

Mailani, G., 2006. Monitoring of Tailing Dams with Geophysical Methods. Luleå University of Technology, Department of Chemical Engineering and Geosciences. Division of Ore Geology and Applied Geophysics. Licentiate Thesis. 74.

Malagutti Filho, W., et al., 2018a. Emprego integrado de métodos sísmicos e geoelétricos no estudo de barragens de terra de pequeno porte. VII Simpósio Brasileiro de Geofísica, Salinópolis.

Malagutti Filho, W., et al., 2018b. Study of small earthfill dams structure using seismic refraction, ert and self-potential methods. In: 24th European Meeting of Environmental and Engineering Geophysics, pp. 1–5, 2018.

Martínez, J., et al., 2021. Characterization of tailings dams by electrical geophysical methods (ERT, IP): Federico Mine (La Carolina, Southeastern Spain). Minerals 11 (2), 145.

Massignan, R.S., Sánchez, L.E., 2022. What does it mean to 'decharacterize' tailings dams? A systematic literature review. Engenharia Sanitaria e Ambiental 27, 225–234.

Melcher, G.C., 1954. Nota sobre o distrito alcalino de Jacupiranga. Estado de São Paulo, DNPM/ DGM, p. 20.

Oliveira, L.A., 2018. Caracterização de barragens de rejeito através de métodos geofísicos elétricos: estudo de caso na barragem B1 de Cajati, São Paulo. Universidade Federal do Rio de Janeiro, Instituto de Geociências, Graduação em Geologia. Trabalho de conclusão de curso. 109 p.

Rey, J., et al., 2021. Assessment of tailings ponds by a combination of electrical (ERT and IP) and hydrochemical techniques (Linares, southern Spain). Mine Water Environ. 40 (1), 298–307.

Rocha, D.C.G., Braga, M.A.S., Rodrigues, C.T., 2019. Geophysical methods for BR tailings dam research and monitoring in the Mineral complex of Tapira - Minas Gerais, Brazil. Brazilian J. Geophys. 37 (3), 275–289.

Rodrigues, C.T., 2018. Geofísica aplicada à investigação de barragem de rejeito BR, do Complexo de Mineração de Tapira, Minas Gerais. Universidade Federal do Rio de Janeiro, Instituto de Geociências, Graduação em Geologia. Trabalho de conclusão de curso. 61 p.

Rotta, L.H.S., et al., 2020. The 2019 Brumadinho tailings dam collapse: possible cause and impacts of the worst human and environmental disaster in Brazil. Int. J. Appl. Earth Obs. Geoinf. 90, 102119.

Sasaki, Y., 1992. Resolution of resistivity tomography inferred from numerical simulation 1. Geophys. Prospect. 40 (4), 453–463.

Scaioni, M., et al., 2018. Geodetic and remote-sensing sensors for dam deformation monitoring. Sensors 18 (11), 3682.

Sentenac, P., et al., 2017. Post flooding damage assessment of earth dams and historical reservoirs using non-invasive geophysical techniques. J. Appl. Geophys. 146, 138–148.

Sentenac, P., Benes, V., Keenan, H., 2018. Reservoir assessment using non-invasive geophysical techniques. Environ. Earth Sci. 77 (7), 1–14.

Sjödahl, P., Dahlin, T., Johansson, S., 2005. Using resistivity measurements for dam safety evaluation at Enemossen tailings dam in southern Sweden. Environ. Geol. 49, 267–273.

Souza, L.A.P., et al., 2016. Contribuição dos métodos geofísicos na construção e monitoramento de barragens. In: III Congresso da Sociedade de Análise de Risco Latino Americana SRA-LA, 2016, São Paulo.

Titov, K., Loukhmanov, V., Potapov, A., 2000. Monitoring of water seepage from a reservoir using resistivity and self-polarization methods: case history of the Petergoph fountain water supply. First Break 18, 432–434.

United Nations Environment Programme, 2020. Global Industry Standard on Tailings Management. Available at: https://wedocs.unep.org/20.500.11822/36139 (Accessed: 30 August 2022).

Vick, S.G., 1990. Planning, design, and analysis of tailings dams. BiTech Publishers Ltd, Vancouver, B.C. Canada, 381 p.